

ARTICLE

Transcriptionally regulated and nontoxic delivery of the hyperactive *Sleeping Beauty* Transposase

Fabienne Cocchiarella¹, Maria Carmela Latella¹, Valentina Basile², Francesca Miselli¹, Melanie Galla³, Carol Imbriano² and Alessandra Recchia¹

The *Sleeping Beauty* (SB) transposase and, in particular, its hyperactive variant SB100X raises increasing interest for gene therapy application, including genome modification and, more recently, induced pluripotent stem cells (iPS) reprogramming. The documented cytotoxicity of the transposase, when constitutively expressed by an integrating retroviral vector (iRV), has been circumvented by the transient delivery of SB100X using retroviral mRNA transfer. In this study, we developed an alternative, safe, and efficient transposase delivery system based on a tetracycline-ON regulated expression cassette and the rtTA2^S-M2 transactivator gene transiently delivered by integration-defective lentiviral vectors (IDLVs). Compared with iRV-mediated delivery, expression of tetracycline-induced SB100X delivered by an IDLV results in more efficient integration of a GFP transposon and reduced toxicity. Tightly regulated expression and reactivation of the transposase was achieved in HeLa cells as well as in human primary keratinocytes. Based on these properties, the regulated transposase-IDLV vectors may represent a valuable tool for genetic engineering and therapeutic gene transfer.

Molecular Therapy — Methods & Clinical Development (2016) **3**, 16038; doi:10.1038/mtm.2016.38; published online 15 June 2016

INTRODUCTION

The “resurrection” of the *Sleeping Beauty* (SB) transposon¹ aroused the interest of the scientific community for its enormous potential as a tool in mammalian genome engineering studies. This interest conveyed in an extensive engineering effort aimed at ameliorating the transposition activity by modifying both components of the SB system, the transposon inverted repeats (IRs) and the transposase enzyme. These efforts resulted in the generation of the hyperactive SB100X transposase² and T2 IRs arrangement modifying the outer and inner Direct repeats (DRs) sites and the spacer sequence between the DRs, showing a fourfold enhanced activity over the standard T IRs³ and the high-capacity “sandwich” IRs (SA),⁴ designed to transpos large DNA fragment (>10 kb). The hyperactive SB100X coupled to the T2-based transposon has been already engaged in preclinical gene therapy applications,^{2,5–7} genome modification^{8–10} and, more recently, iPS reprogramming.^{11–13} Typically, the SB transposase is provided transiently by plasmid transfection to prevent remobilization of the transposon integrated into the human genome,¹⁴ and its expression is usually driven by a strong constitutive promoter, e.g., the cytomegalovirus (CMV) promoter. Since overproduction inhibitory effects have been reported,^{15,16} a careful molar balance between the transposase and the transposon is required for optimal transposition. However, despite the improved new methods of transfection, delivery of the two-component system remains a challenge for many applications. In particular, nonviral delivery methods are not suitable for primary cells such as keratinocytes, hepatocytes or photoreceptor cells that are refractory to transfection, thus developments of new delivery system gained increasing

interests. Besides conventional transfection methods for plasmid and mRNA coding for transposase,^{17,18} viral delivery based on adenoviral,^{19,20} AAV,²¹ Baculovirus,²² gammaretroviral,²³ and lentiviral²⁴ vectors has been proposed in the past. The use of integrating gammaretroviral and lentiviral vectors as vehicles for transposase delivery raise safety concerns due to the risk of uncontrollable rehousing of the transposon as a result of stable expression of the transposase. This can be circumvented by the use of shorter lived mRNA packaged into retrovirus particles;²³ or of integration-defective LVs carrying expressing SB11 transposase;²⁵ or the hyperactive version SB100X.²⁴ More recently, several in depth analyses about the rates on insertional mutagenesis and remobilization showed that they occurred infrequently.²⁶

Alternatively, transcriptional regulation based on Tet-On system is widely used to control gene expression. The system, originally developed by Gossen and Bujard more than 20 years ago (1992), has undergone several refinements aimed to improve the efficacy limiting the leakiness of the transcription level in absence of the inducer. These modifications have included improvements of the Tet-responsive promoter obtained by substituting the minimal CMV promoter fused to the TetO₇– element with the minimal promoter (-81) of the HSV-1 thymidine kinase (*TK*) gene²⁷ or by introducing a short (36 nt) spacing between two consecutive TetO sites and increasing the number of TetO sites from 7 to 8.²⁸ In 2000, a new transcriptional modulator, rtTA2^S-M2, was generated by replacing the full-length VP16 transcriptional activation domain by a full codon optimized domain derived from VP16 itself.²⁹ This Tet-On variant was successfully used for *ex vivo* and *in vivo* delivery of tetracycline-regulated genes.^{30,31} In this study,

¹Department of Life Sciences, Centre for Regenerative Medicine, University of Modena and Reggio Emilia, Modena, Italy; ²Department of Life Sciences, University of Modena and Reggio Emilia, Modena, Italy; ³Institute of Experimental Hematology, Hannover Medical School, Hannover, Germany. Correspondence: A Recchia (alessandra.recchia@unimore.it) Received 21 January 2016; accepted 21 April 2016

we took advantage of this new system to develop an efficient, safe, and transcriptionally regulated transposase delivery platform based on the Tet-On regulatory system and on integration-defective lentiviral vector (IDLV). We generated two IDLV vectors, one carrying the rtTA2^S-M2 transactivator and the second bearing the tightly regulated, drug-inducible SB100X expression cassette. The combination of the two vectors resulted in a strong reduction of background expression in the off-state and in a high induction of transposase expression upon doxycycline (dox) treatment. Before addressing the potential cytotoxic side-effects of the Tet-regulated SB100X carried by an IDLV in comparison to the constitutively expressed SB100X delivered by a gammaretroviral vector (iRVSB) or by lentiviral vector (IDLVSB). We showed that dox-induced or constitutively expressed SB100X expression in IDLV did not affect cell proliferation, and did not trigger DNA damage response or apoptosis, in contrast to iRVSB, which induces a G2/M arrest and apoptotic cell death even in the absence of a cotransfected transposable element. Comparing the IDLV transposase delivery platform with the iRVSB vector, we found that expression of dox-induced or constitutively expressed SB100X delivered by IDLVs gave rise to more efficient integration of a sandwich GFP transposon (pSAGFP)^{4,32} in HeLa cells in absence of selection. We showed significant regulation of SB100X expression upon dox treatment in human primary keratinocytes resulting in a transposition of the GFP reporter gene in keratinocytes cultivated *in vitro* on 3T3 feeder layer.

Thus, the dox-induced transposase IDLV platform that combines the efficiency and the transcriptional regulation of SB100X represents a promising application in human primary cells.

RESULTS

Transcriptional regulation of the hyperactive SB transposase

To overcome the cytotoxic effects of the constitutive expression of the SB100X delivered by an integration competent retroviral vector, we developed two alternative constructs, in which the expression of the transposase was controlled by a tetracycline-inducible activation system. The pTetOCMVSB and pTetOTKSB plasmids contained the SB100X expression cassette under the control of the CMV immediate-early minimal promoter (-53) or the minimal promoter (-81) of the HSV-1 gene *TK* linked to the bacterial Tet operator (TetO). The tetracycline controlled reverse transcriptional activator (rtTA2^S-M2)²⁹ was expressed under the control of the phosphoglycerate kinase (PGK) promoter (Figure 1). In the presence of the inducer, the tetracycline analogue dox, the rtTA2^S-M2 protein allows activation of TetO-CMV or TetO-TK transcription. The control CMVSB plasmid contained the transposase expression cassette driven by the CMV promoter/enhancer (Figure 1).

Regulated expression of the transposase and transposition of a sandwich transposon carrying a PGK-driven GFP cassette (pSAGFP)³² (Figure 1) were assessed by cotransfecting HeLa cells with pSAGFP and pCMVSB or pSAGFP and pTetOTKSB or pTetOCMVSB alone and in combination with pPGKrtTA2^S-M2 in the presence and absence of dox. As control, HeLa cells were transfected with the pSAGFP alone. Half of the cells were harvested 48 hours after transfection, and their mRNA analyzed for SB100X expression by real time qRT-PCR. The increased transposase expression in the activating conditions (plus rtTA2^S-M2 and \pm dox) was measured over the background (pTetOTKSB and pTetOCMVSB alone). As shown in Figure 2a,b pronounced activation (16 fold in presence of dox) of transposase expression was achieved in the cells co-transfected with pTetOTKSB and pPGKrtTA2^S-M2 plasmids compared to the cells that received only pTetOTKSB. A robust activation (71 fold in presence of dox) but

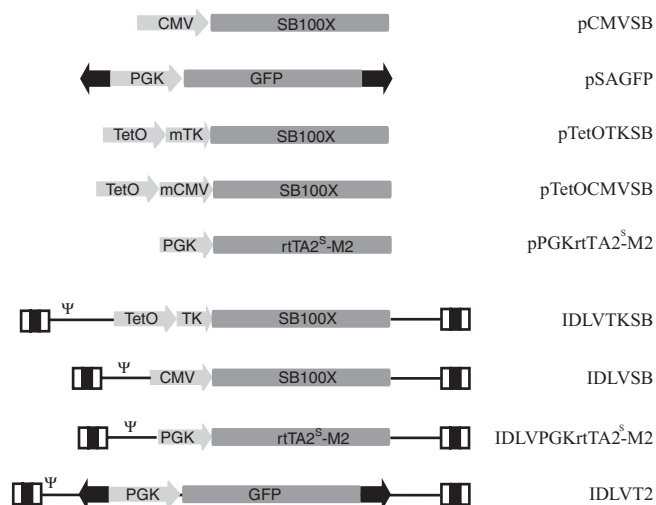


Figure 1 Schematic outline of the plasmids and viruses carrying transposon or transposase. pCMVSB carries the SB100X transposase coding sequence placed under the control of the cytomegalovirus (CMV) promoter. The sandwich GFP transposon (pSAGFP) carries the GFP under phosphoglycerate kinase (PGK) promoter embedded in SA transposon. The plasmids pTetOTKSB and pTetOCMVSB carry the transposase under the Tet operator (TetO) and the minimal TK (mTK) or minimal CMV promoter (mCMV), respectively. The plasmid pPGKrtTA2^S-M2 codes for the rtTA2^S-M2 transactivator transcribed from PGK promoter. Black arrows represent the transposon IRs. All the IDLV vectors (IDLVTKSB, IDLVSB, and IDLVrtTA2^S-M2) were obtained by cloning the transposase and transactivator expression cassettes described above into nonintegrating lentiviral vector. Lastly the IDLVT2 vector carries the GFP reporter gene driven by the PGK promoter embedded in T2 transposon. All the expression cassettes carry the SV40 poly-Adenylation signal (not shown). The constructs are not in scale. PGK, phosphoglycerate kinase; TK, thymidine kinase promoter; IDLV, integration-defective lentiviral vectors.

more leaky SB100X expression (sevenfold in absence of dox) was measured in the cells cotransfected with the pTetOCMVSB and the pPGKrtTA2^S-M2 compared with the cells in absence of the activator. The cells were kept in culture to perform a transposition experiment aimed at the identification of integration efficiency of the IR flanked transgene without any selective pressure. At least three independent experiments for each regulated transposase were performed in order to reduce variability due to transfection procedure. We determined also by qPCR the copy number of transposon and transposase plasmids in HeLa cells 2 days post-transfection (see Supplementary Figure S1). The copy number of GFP transposon was pretty comparable among the TetOTK and TetOCMV cotransfected samples; whereas SB100X copy number in pCMVSB sample was lower than all the other SB-transfected samples nevertheless it showed a high SB100X expression (see Supplementary Figure S2).

Transgene expression during the culture period (up to 20 days) was measured by FACS to determine the percentage of GFP⁺ cells that, at the endpoint of culture, harbored at least one copy of transposon expressing GFP per cell (see Supplementary Figure S3). Figure 2b shows on the Y-axis the %GFP⁺ cells 20 dpt / %GFP⁺ cells 2 dpt \times 100 for each sample. The percentage corresponding to the pSAGFP sample alone (on average of 0.7%) was subtracted to the percentage deriving from SB-treated sample. The TetO-TK promoter resulted in a ratio of GFP⁺ cells of 56% with respect to the TetO-CMV promoter (78%) even in absence of the activator. A mild induction upon dox addition (63%) was detected with the TetOTKSB plasmid compared with 10% measured with the TetO-CMV regulated transposase in presence of dox, probably due to overproduction

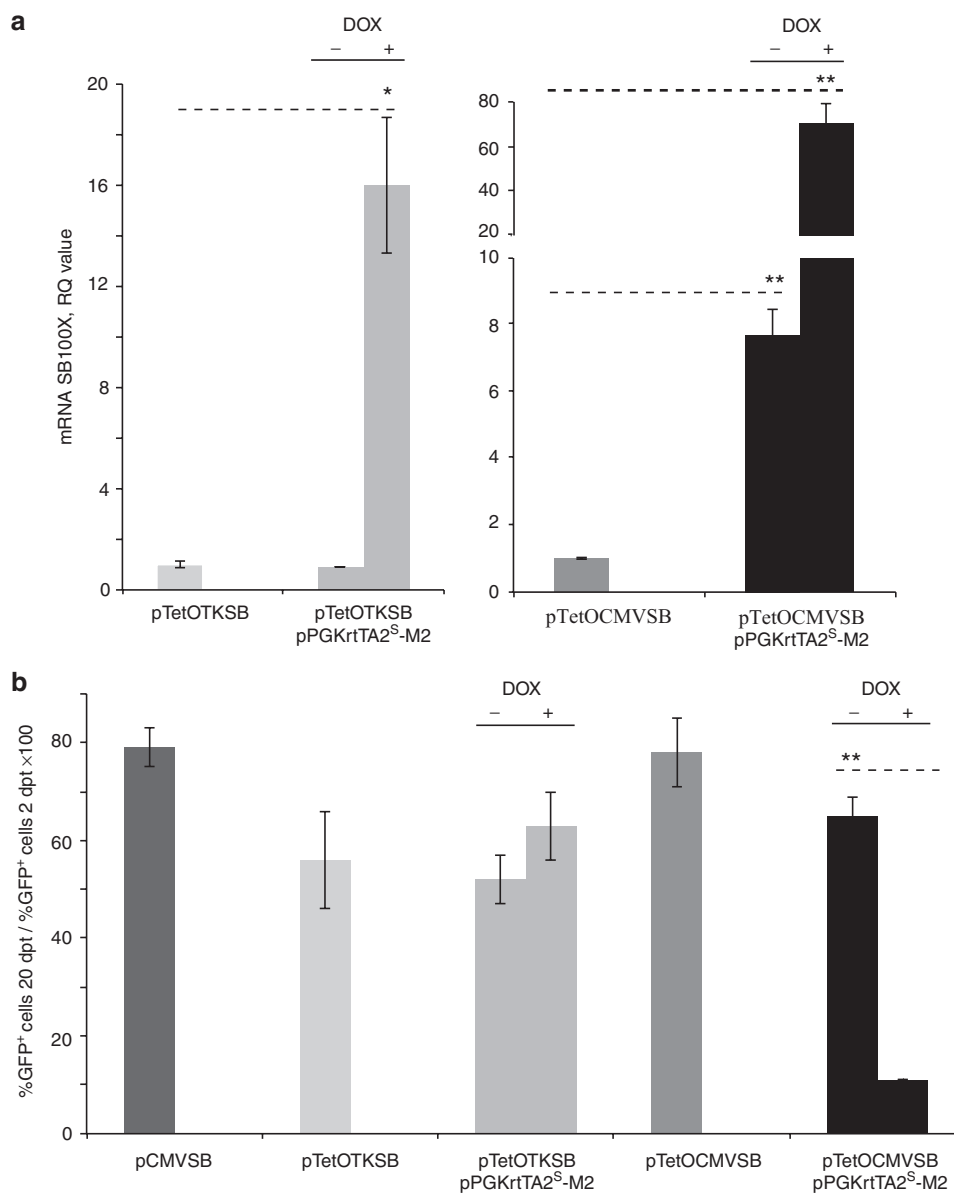


Figure 2 Sleeping Beauty (SB) transposase expression and activity from Tet-On transcriptionally regulated plasmids. (a) Quantitative reverse-transcriptase polymerase chain reaction (qRT-PCR) assay on the transposase expression. HeLa cells were transfected with pTetOTKSB and pTetOCMVSB alone or in combination with pPGKrtTA2^S-M2 in presence and in absence of dox. Transposase expression was measured by Taqman RT PCR and plotted as RQ value with respect to the off state (pTetOTKSB and pTetOCMVSB alone, RQ value = 1). The experiment was performed in triplicate and is presented as mean value \pm standard error of the mean (SEM). Dashed lines connect samples showing significant different values (* $P < 0.1$, ** $P < 0.05$). (b) HeLa cells were cotransfected with the transposase coding plasmids described above and the pSAGFP transposon. As positive control a constitutive expression of the transposase provided by the pCMVSB plasmid was used. The experiment was performed in triplicate and on the Y-axis is presented %GFP⁺ cells 20 dpt / %GFP⁺ cells 2 dpt $\times 100$ (mean \pm SEM). Dashed lines connect samples showing significant different values (** $P < 0.05$)

inhibition (Figure 2b). These data clearly indicate the superior regulatory property of the TetO-TK promoter and the fateful effect of regulation of the transposase activated by TetO-CMV promoter, therefore the TetO-TK configuration was chosen to regulate the SB100X transposase. A more controlled delivery of the two Tet-components could allow a fine regulation of transposase expression avoiding overproduction inhibition and toxicity.

Nonintegrating lentiviral-based transposase activity.

In order to get transposition in primary cells that are refractory to physicochemical transfection, *i.e.*, keratinocytes, we incorporated the transposase into integration-defective lentiviral vector (IDLV).

To overcome cytotoxic effects of constitutive expression of the transposase carried by IDLV that could persist in the genome of the target cells due to residual integration activity, we developed two IDLVs expressing the TetO-TK regulated transposase (IDLVTKSB) and the reverse transactivator rtTA2^S-M2 (IDLVrtTA2^S-M2) (Figure 1). We also introduced the 900bp Woodchuck Hepatitis Virus post-transcriptional regulatory element (WPRE)³³ at the 3' end of the SB100X cDNA to possibly increase mRNA processing and stability. IDLV particles pseudotyped with the Vesicular Stomatitis Virus glycoprotein (VSV-G) were packaged, concentrated and measured by HIV-1 Gag p24 immunocapture. To determine the most efficient vectors dose combination, we performed a dose escalation experiment

transducing HeLa cells with increasing doses (130, 260, and 2,600 ng p24) of IDLVTKSB in combination with IDLVrtTA2⁵-M2 (960 and 9,600 ng p24), in presence and in absence of dox. Nice activation of the transposase was measured in all conditions (see Supplementary Figure S4) although higher dose of IDLVTKSB was required to obtain approximately eightfold activation of SB100X expression over the background, as shown in the qRT-PCR analysis (IDLVTKSB alone) (Figure 3a). To easily compare the qRT-PCR data on SB100X expression obtained with plasmid with those from viruses, we merged the data in Supplementary Figure S2.

For some gene therapy purposes, iPS reprogramming or generation of cell lines stably and highly expressing the gene of interest, a fast clearance of transposase or multiple transposition events are desired. Cellular reprogramming based on SB system represents a novel, viable and safe approach of generating iPS cells.¹¹ Grabundzija *et al.* clearly showed the presence of iPS cell colonies 3 days post-transposase's delivery, indicating that the activity of SB100X was carried out and its expression would no longer be required. Thus a transcriptional silencing of transposase expression, that could follow a different timing in different cell,³⁴ could be desired and benefit the iPS colonies formation and growth. The generation of stable cell line for viral production could require more than one copy of the packaging genes. To increase the copy number and the expression of the packaging genes, multiple rounds of transposon/transposase delivery could be required. Thereby drug-inducible reactivation of the transposase provided in the first round will limit the readministration of the two-components system to the transposon plasmid.

Thus, we asked whether the transcriptionally controlled SB100X, expressed by the combination of two IDLVs, could fulfil the quick down-regulation of transposase expression upon dox withdrawal and its reactivation upon dox treatment, so that multiple transduction cycles that could exhaust primary cells limiting their clonogenic potential, *e. g.*, keratinocytes, are avoided.

We followed the switching of the on and off-state of transposase expression by semi-quantitative RT-PCR assay on mRNA purified from transduced HeLa cells. The transposase expression over time, at the indicated time points, was calculated upon GAPDH normalization and plotted as SB100X mRNA fold change respect to highest transposase expression level (value = 1) achieved 48 hours post-transduction upon dox treatment (Figure 3b). We transduced HeLa cells with IDLVTKSB (2,600 ng p24) and IDLVrtTA2⁵-M2 (9,600 ng p24) in absence and in presence of dox (black and light gray line, respectively). Two days post-transduction we extracted the mRNA to perform the RT-PCR and we split the bulk activated by dox for 48 hours in two sub-populations, in the bulk A (light gray line) we readministered the dox whereas in the other bulk the dox was not added (bulk B) (dashed line). Five days post-transduction, in the bulk A, kept constantly in presence of dox, SB100X expression is clearly detected compatible with the dilution of the IDLVTKSB vector in actively replicating HeLa cells. Conversely, we observed an almost complete shut off of transposase expression 3 days post dox withdrawal, 5 days post-transfection (5 dpt) in the bulk B (dashed line). Interestingly, the SB100X expression was rescued 2 days after the readministration of dox for 48 hours (7 dpt) (dotted line) in the bulk B, reaching at day 9, a level comparable to the permanently activated SB100X expression (light gray line) (bulk A). RT-PCR assay performed 12 and 20 dpt on the reactivated and the permanent activated sub-populations respectively, showed no SB100X expression, consistently with the almost undetectable IDLVTKSB vector in the HeLa genome (see Supplementary Figure S5).

We also evaluated the integration of a GFP transposon mediated by the regulated SB100X in comparison to a constitutively expressed SB100X carried by IDLV (IDLVS) (Figure 1) and by a gamma retroviral vector (iRVSB).²³ HeLa cells were transfected with the pSAGFP transposon and 16 hours later were transduced with IDLVrtTA2⁵-M2 (9,600 ng p24) and IDLVTKSB (260 and 2,600 ng p24 doses) vectors in presence and in absence of dox and with the constitutively SB100X expressing vectors, IDLVS and iRVSB. We evaluated the copy number of pSAGFP transposon and SB transposase by qPCR 2 days post-transfection/transduction (see Supplementary Figure S6). The copy number of the SB transposase carried by dox-regulated IDLV vector was related, not surprisingly, to the amount of IDLVTKSB virus delivered (260 ng or 2,600 ng p24) to the cells, however the copy number in the samples \pm dox was comparable. The SB100X copy number in iRVSB-treated sample is lower than all other SB vectors in particular the IDLVTKSB (2,600 ng p24)+IDLVT2A2M2-treated sample although they sustained comparable transposition of GFP cassette delivered with comparable efficiency (see Supplementary Figure S7). The activity of iRVSB is presumably ascribed to the robust SB100X expression measured by qRT-PCR (see Supplementary Figure S2). Expression of the GFP was traced every 6 days for a total of 21 days (see Supplementary Figure S7). The %GFP⁺ cells 21 dpt / %GFP⁺ cells 2 dpt \times 100 was 78% with the high dose of regulated SB vector compared with 58% and 76% scored with the iRVSB and IDLVS vector respectively. Low dose of the IDLVTKSB in combination with IDLVrtTA2⁵-M2 vector reached 42% upon dox activation. As performed for the cotransfection experiment in Figure 2b, the %GFP⁺ cells 21 dpt / %GFP⁺ cells 2 dpt \times 100 for each sample was normalized to the transposon alone (on average of 0.58%) (Figure 3c). Interestingly, this condition resulted in fivefold increase of GFP⁺ cells in the ON state and in poor (9%) transposase activity when the dox is not added to the cell culture.

Transcriptionally regulated transposase delivered by IDLV is not cytotoxic

To investigate whether Tet-regulated transposase could affect cell proliferation, we performed a Crystal Violet (CV) assay on HeLa cells transduced with high doses of IDLVTKSB and IDLVrtTA2⁵-M2 vectors and with the constitutively SB100X expressing vectors, iRVSB and IDLVS. As control we generated an IDLVNC and iRVNC vectors carrying a PGK-GFP expression cassette. Analyzing the absorbance ($A_{540\text{ nm}}$) 48, 72, 96, and 120 hours post-transduction in all sample treated, we observed a modest but not significant decrease in cell proliferation following dox-induced SB100X expression in the sample cotransduced with IDLVTKSB-IDLVrtTA2⁵-M2 respect to the IDLVNC, particularly at 120 hours post-transduction. At the above time point, the comparison between cells transduced with iRVNC and IDLVs vectors, and between IDLVS and IDLVNC, did not show significant differences in cell growth. Differently, iRVSB caused an evident and irreversible inhibition of cell growth, already marked at 72 hours post-transduction (Figure 4a).

Propidium-iodide (PI) monoparametric cell cycle analysis was then performed by flow cytometer at 72 hours post-transduction (Figure 4b). No differences were detected in the distribution of cell populations throughout the different phases of the cell cycle following activation of SB100X expression (compare IDLVTKSB-IDLVrtTA2⁵-M2 vs. IDLVTKSB-IDLVrtTA2⁵-M2+dox). Same behavior was observed in the IDLVS transduced cells. In contrast, iRVSB transduction accumulated the cells in the G2/M phase (from 21% of iRVNC to 53% of iRVSB cells), to the detriment of G0/G1 population,

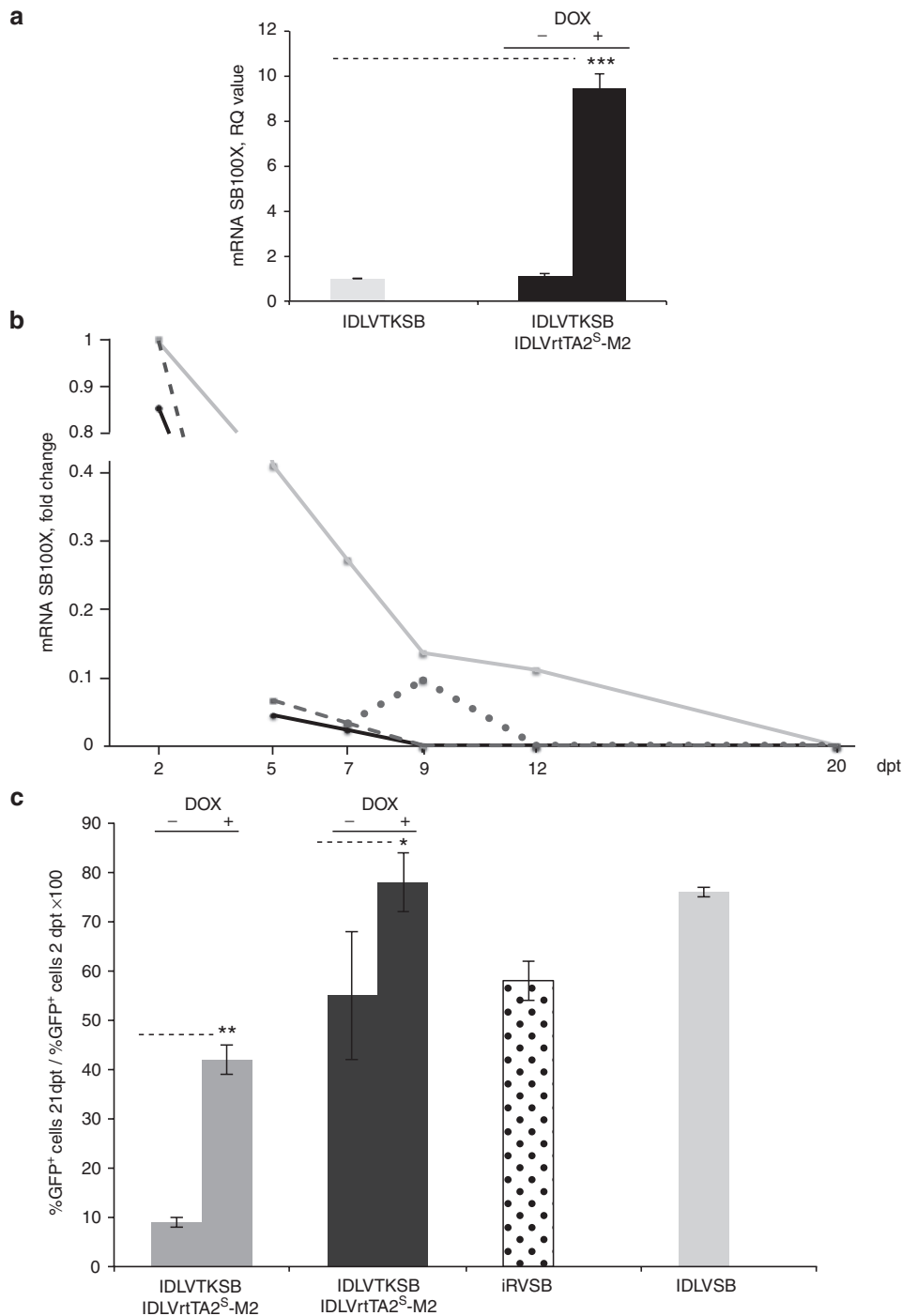


Figure 3 Transcriptionally regulation and transposition mediated by Sleeping Beauty (SB) transposase carried by IDLV vectors. **(a)** qRT-PCR assay on HeLa cells transduced with IDLVTKSB (2,600 ng p24) in presence or in absence of IDLVrtTA2^S-M2 (9,600 ng p24) and dox. Transposase expression upon activation was measured by real time Taqman RT-PCR and plotted as RQ value with respect to the off state (IDLVTKSB alone, RQ value = 1). The experiment was performed in triplicate and is presented the mean ± SEM. Dashed lines connect samples showing significant different values (***) $P < 0.005$ **(b)** On and off state of the transposase expression. A time course experiment (2, 5, 7, 9, 12, and 20 days post-transduction, dpt) was performed in HeLa cells cotransduced with the IDLVTKSB (2,600 ng p24) and IDLVrtTA2^S-M2 (9,600 ng p24). Light gray and black lines represent cells cultivated in presence and in absence of dox, respectively. Dashed line represents the effect of dox withdrawal up to 20 dpt. Dotted line shows the effect of readministration of dox 7 dpt. **(c)** HeLa cells were transduced with the pSAGFP transposon and transduced with the IDLVTKSB (260 ng p24 and 2,600 ng p24; gray and black bars respectively) and IDLVrtTA2^S-M2 (9,600 ng p24) in presence and in absence of dox and compared with the iRVSB (dotted bar) and IDLVSB (light gray bar) vectors. The experiment was performed in triplicate and on the Y-axis is presented the %GFP⁺ cells 21 dpt / %GFP⁺ cells 2 dpt × 100 (mean ± SEM). Dashed lines connect samples showing significant different values (* $P < 0.1$, ** $P < 0.05$). qRT-PCR, quantitative reverse-transcriptase polymerase chain reaction; IDLV, integration-defective lentiviral vector; pSAGFP, sandwich GFP transposon; SEM, standard error of mean.

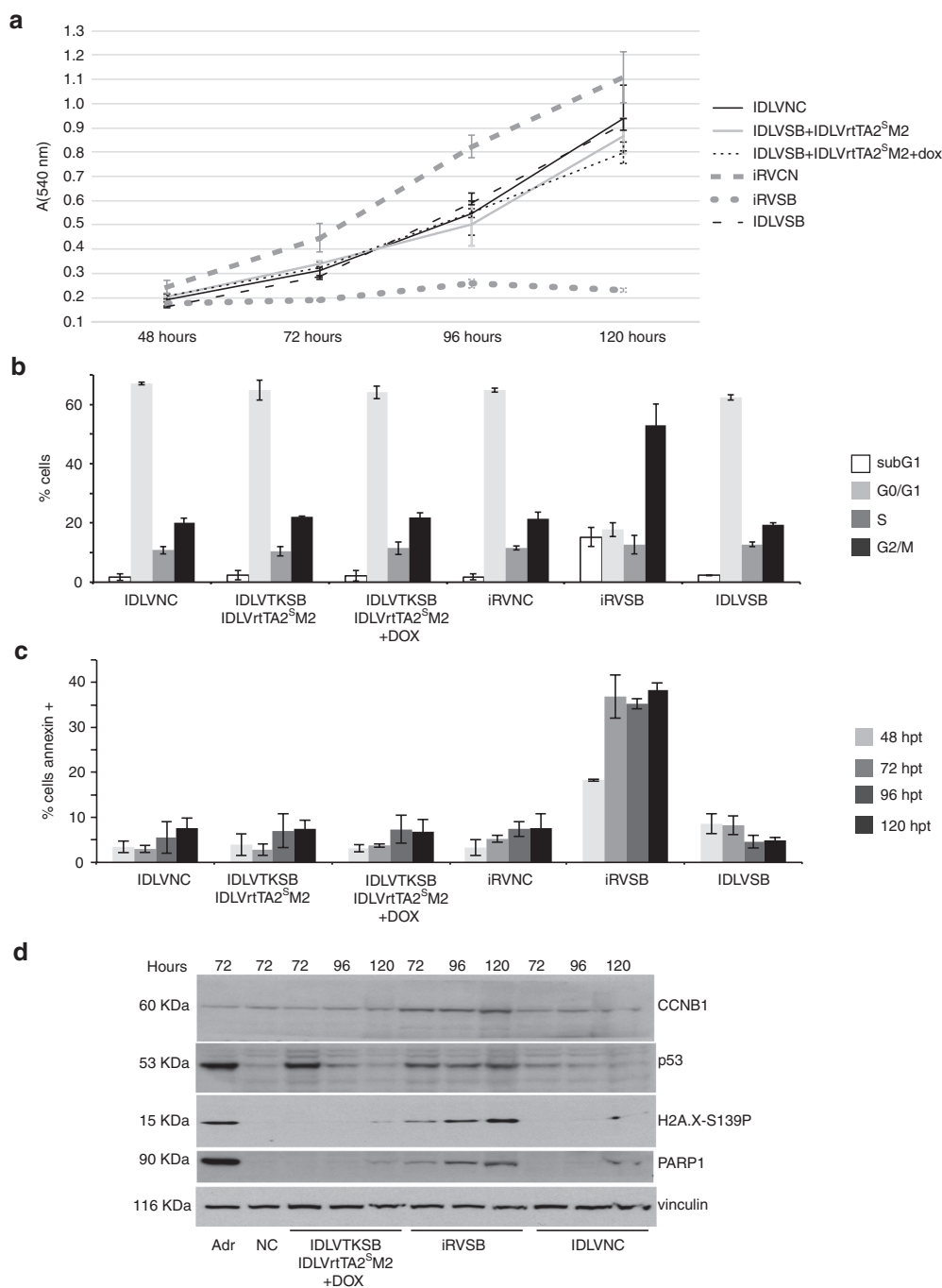


Figure 4 Effects of transcriptionally regulated expression of Sleeping Beauty (SB) transposase on cell viability and proliferation. **(a)** Proliferation rates of HeLa cells transduced with the indicated vectors by absorbance measurement (A_{540nm}) of crystal violet staining at 48, 72, 96, and 120 hours post-transduction (hpt). **(b)** Distribution of transduced cells (% cells) throughout the different phases of the cell cycle at 72 hours post-transduction, as measured by PI-cytometer analysis of DNA content. **(c)** Percentages of cells positive to AnnexinV staining at the indicated time points (hpt). The experiments in panel **a**, **b**, **c** were performed in triplicate and are presented as mean \pm SEM. **(d)** Western blot analysis of CCNB1, p53, H2AX-S139P and cleaved-PARP1 expression in total extracts from IDLVTKSB+IDLVrtTA2^S-M2 +dox, iRVSB and IDLVNC transduced cells at the indicated time points. Adriamycin (Adr) was used as positive control for DNA damage and apoptosis activation. Signals were normalized with a polyclonal antibody against the vinculin. PI, Propidium-Iodide; SEM, standard error of mean.

as already described by Galla *et al.*²³ and the percentage of SubG1 cells raised from 2.5% (iRVNC) to 18% (iRVSB).

Although no increase of SubG1 events was detected by PI flow cytometer analysis in IDLVrtTA2^S-M2 cells, we further investigated whether dox-induced SB100X could activate an apoptotic response. The Annexin-V assay, which detects externalized phosphatidylserine (PS) at the plasma membrane, was used to evaluate early apoptosis

(Figure 4c). The percentage of Annexin-V positive cells detected following time-course incubation of IDLVTKSB- IDLVrtTA2^S-M2 with dox was comparable with control cells (IDLVTKSB- IDLVrtTA2^S-M2). Differently, constitutive SB100X expression by gammaretroviral vector (iRVSB) showed an evident increase of Annexin-V staining for all the time points analyzed. Conversely IDLVSB vector behaves similarly to the IDLVNC control.

Finally, we analyzed by Western Blot the expression of key proteins involved in cell cycle progression and apoptotic response. As shown in Figure 4d, the levels of CyclinB1 (CCNB1), which controls the G2 to M progression, were not affected by dox-induced SB100X expression, while an increase was observed in iRVSB transduced cells, consistent with the accumulation G2/M events (Figure 3b). Compared with control cells, the expression of the tumor suppressor p53, regulator of cell proliferation and apoptosis, rose at 72 hours post-transduction in IDLVTKSB-IDLVrtTA2⁵-M2+dox cells, and then decreased to control levels at 120 hours, hinting at a reversible activation of p53 induced by dox treatment. Differently, constitutive SB100X expression led to a long-term increase of p53, presumably involved in cell cycle arrest and cell death mechanisms. To corroborate that Tet-regulated SB100X did not activate DNA damage and apoptosis, in opposition to iRVSB, we analyzed the expression of γ H2AX-S139P, H2AX histone variant phosphorylated at Ser139 in response to DNA damage, and cleaved-PARP1, hallmark of apoptosis. As expected, their expression levels were increased by iRVSB, but no changes were observed following dox-induced SB100X activation, compared with IDLVNC.

Overall, these data demonstrate that Tet-regulated transposase expression has no cytotoxic effects and could therefore be used to mediate transposition in human primary cells.

Transcriptional regulation of SB transposase in human primary cells
The efficacy of the regulated transposase coupled to its nontoxic effect prompted us to investigate its activity in human primary keratinocytes. We firstly evaluated the transcriptional response to dox treatment. We cotransduced human primary keratinocytes with IDLVTKSB and IDLVrtTA2⁵-M2 in the presence and absence of dox and as control with IDLVSB. The qRT-PCR analysis on transposase expression 5 dpt showed a 15-fold transcriptional activation over the uninduced cells and a level of SB100X expression comparable to the IDLVSB vector where transposase is driven by the constitutive CMV promoter (Figure 5a).

To perform transposition experiments, human primary keratinocytes were co-transduced with IDLVT2 alone or in combination with IDLVTKSB+IDLVrtTA2⁵-M2 in presence or absence of dox or with IDLVSB and kept in culture on irradiated 3T3 feeder layer for 5 days, without selective pressure. Transgene expression was measured by flow cytometer analysis to determine the percentage of GFP⁺ cells 2 days post-transduction and at the endpoint of culture (5 days), when the transposon alone drops to barely undetectable level (on average of 0.6%) (see Supplementary Figure S8a). The ratios between the percentage of GFP⁺ cells at the endpoint and the percentage of GFP⁺ cells 2 days post-transduction, normalized to the transposon alone, is shown in Figure 5b. To investigate whether Tet-regulated transposase vector could affect cell viability, 1.6 × 10⁵ keratinocytes transduced with IDLVT2 in combination with IDLVTKSB and IDLVrtTA2⁵-M2 or with IDLVSB were counted 2 days post-transduction. We observed a reduction on keratinocytes viability in the samples transduced with 3 IDLV vectors (IDLVT2, IDLVTKSB, and IDLVrtTA2M2) respect to IDLVT2 ± IDLVSB-transduced cells 48 hours post-transduction (see Supplementary Figure S8b), probably related to the total viral load since after day 2 all the samples underwent comparable cell growth (data not shown). To improve the system, we incorporated the TetOTK-regulated SB100X in the rtTA2⁵-M2 transactivator vector generating the IDLVTKreg vector (see Supplementary Figure S9a). Firstly we assessed the transcriptional activation of the all-in-one vector (IDLVTKreg) upon dox treatment. We transduced human primary keratinocytes with

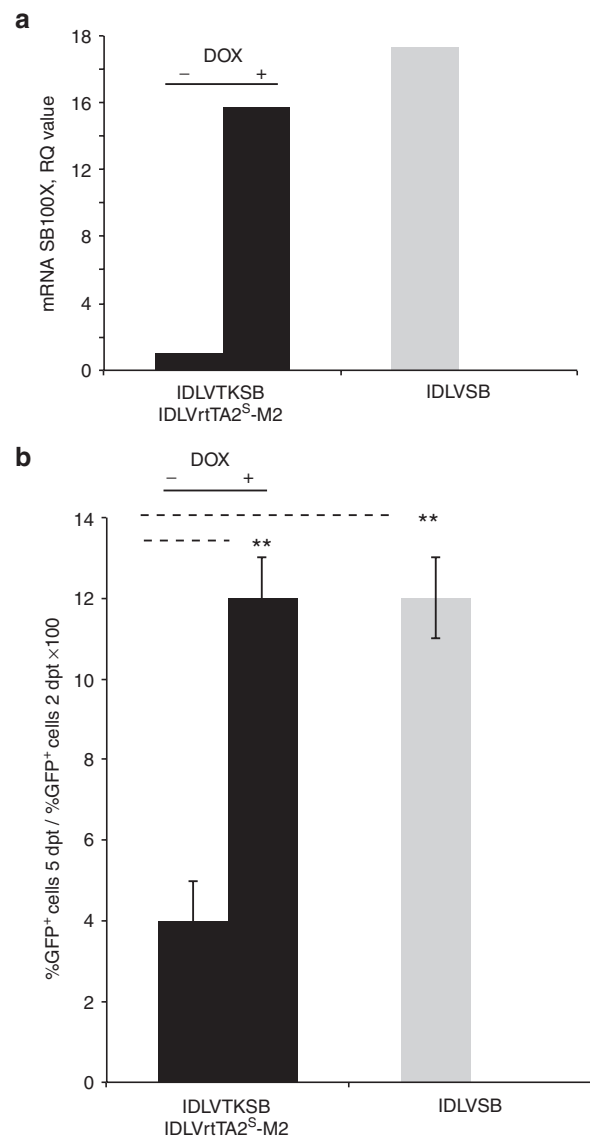


Figure 5 Transcriptionally regulated and Sleeping Beauty (SB)-mediated transposition in human primary keratinocytes. **(a)** qRT-PCR assay on primary keratinocytes transduced with IDLVTKSB and IDLVrtTA2⁵-M2 in presence or in absence of dox compared to the IDLVSB. **(b)** Primary keratinocytes were cotransduced with the IDLVT2 transposon, IDLVs transposase vectors in absence and in presence of dox. The experiment was performed in duplicate and on the Y-axis is presented the %GFP⁺ cells 5dpt / %GFP⁺ cells 2 dpt × 100 (mean ± SEM). Dashed lines connect samples showing significant different values (***P* < 0.05). qRT-PCR, quantitative reverse-transcriptase polymerase chain reaction; IDLV, integration-defective lentiviral vector; SEM, standard error of mean.

IDLVTKreg, IDLVTKSB+IDLVrtTA2⁵-M2 in the presence and absence of dox. The qRT-PCR analysis on SB100X expression 5 dpt showed a 10-fold transcriptional activation of the IDLVTKreg vector over the uninduced cells (IDLVTKreg -dox) (see Supplementary Figure S9b). Then, we assessed the transposition of Tet-regulated IDLV vectors in human primary cells. Primary keratinocytes were co-transduced with IDLVT2 alone or in combination with IDLVTKreg in presence or absence of dox and kept in culture on irradiated 3T3 feeder layer for 5 days, without selective pressure. Unfortunately the residual level of GFP⁺ cells in the IDLVTKreg+IDLVT2-treated samples, either in presence or in absence of dox, was below 1% and comparable with the IDLVT2-treated sample (data not shown). These results indicate

that the all-in-one vector did not ameliorate the integration of GFP transposon in this experimental setting. In summary, our findings demonstrated that the hyperactive SB transposase packaged into IDLV particles is transcriptionally regulated, nontoxic, and possess gene transfer potential in human primary cells as needed for potential gene therapy applications.

DISCUSSION

This study presents an efficient, transcriptionally regulated and nontoxic IDLV platform for the delivery of Sleeping Beauty transposase and transposon. Although the SB system¹ was resurrected to provide a nonviral method for introducing defined DNA sequences into vertebrate chromosomes, an efficient delivery of the integration machinery is mandatory to achieve long lasting transgene expression in cycling target cells, as recently shown by the successful use of integrating lentiviral vectors in clinical applications.^{35–38} More recently, the SB system was applied to the engineering of T-cells with a chimeric antigen receptor (CAR) in order to redirect T-cell specificity.^{39,40} In this specific context, nucleofection technique was used to deliver the transposase SB11 plasmid and the transposon plasmid carrying a CD19-specific CAR to the T-cells.⁴¹ To extend the use of the SB system to hardly transfectable primary cells (*e. g.*, keratinocytes and photoreceptor cells) and evaluate its performance in many settings, it is crucial to expand the range of cellular delivery tools for the SB components. In the last years, examples of incorporation of the SB components into viral vectors to take advantage of the viral cell entry properties are numerous.^{20,21,24,25} None of them, however, addressed the issue of the controlled expression of the transposase into the target cells. For some gene therapy applications, such as iPS reprogramming or generation of SB-mediated genetic modification, a quick clearance of transposase or its guided reactivation to get multiple transposition events is desired.

This study introduces the Tet-On-mediated transcriptional regulation of transposase provided by a combined IDLVs platform. We generated two IDLV vectors, one carrying the SB100X transposase under the minimal TetO-TK promoter and the second carrying the reverse transactivator rtTA2^S-M2 under the constitutive PGK promoter. We were able to improve the regulatory performance by replacing the minimal CMV with the minimal TK promoter and by fine tuning the transposase activation over the background expression in the off state by an appropriate vector dose combination. Coupled to a tight regulation of the SB100X transposase, we reported the possibility to switch on and off its expression during time, up to the dilution of the nonintegrating IDLV vectors during cell division. As shown in Figure 3b, 7 days post-transduction, readministration of dox in the IDLVs cotransduced bulk population triggered transposase expression to a level compared with that observed in the cells continuously kept in the presence of dox. Although we used the high transposase vector dose (2,600 ng p24), a complete clearance of SB100X expression was obtained 3 days after dox withdrawal or 20 dpt in the continuously dox-treated sample due to complete dilution of the IDLV episomes. The dynamic range and Tet-regulation could be important in iPS reprogramming where a fast down-regulation of SB100X expression is desired to avoid uncontrolled mobilization of the reprogramming transposon vector. Conversely, the possibility of reactivating the residual transposase episomes later on could be really appreciated during the generation of a stable cell line, *i.e.*, packaging cells for viral vectors or cell line stably expressing a gene of interest. In these cases, multiple transposition events are required and readministration of only one component, the transposon, is preferred particularly when a viral delivery is chosen.

We evaluated the transposition rate of the regulated-IDLVs platform compared with the iRVSB and IDLVSB vector. Transposition of the SAGFP cassette from a plasmid substrate results in higher frequency of genomic integration when Tet-regulated transposase system is provided. Not surprisingly, we observed that the efficiency of transgene insertion into the genome due to SB transposase-mediated integration was vector dose-dependent. High dose of IDLV vectors in presence of dox resulted in high mRNA expression, thus in high number of cells that integrate at least one transposon (78%). In contrast, lower IDLVs doses led to remarkably lower background of transposase expression in the off state and a relevant induction of transposition in presence of the drug.

However, the correlation between transposase expression and number of cells that integrated at least one copy of transposon is not linear, in particular in HeLa cells transfected with pTetOCMVSb+pPGKrtTA2^S-M2 in presence of dox and in cells transduced with iRVSB, where overproduction inhibition coupled to cytotoxicity may limit the transposition rate.

The cytotoxic effects of the Tet-regulated transposase system were investigated by comparing the high doses-IDLVs platform with an integration competent retroviral vector carrying the constitutively expressed SB100X. As previously reported,²³ the iRVSB showed heavy apoptotic effects on a bulk population of transduced HeLa cells, while IDLV-regulated transposase expression did not affect cell viability. The modest decrease of the proliferation rate observed in IDLVTKSB-IDLVrtTA2^S-M2 cotransduced cells in presence of dox compared with its control (IDLVTKSB-IDLVrtTA2^S-M2 w/o dox) could be ascribed to dox administration to the cells. Indeed, it has been shown that dox at the concentration of 1 µg/ml can reduce cell proliferation of multiple human cell lines, included HeLa cells.⁴² The transient increase in the expression of p53, a tumor suppressor involved both in cell cycle arrest and in apoptosis mechanisms, could be one of the causes of the observed delay in cell growth. Despite this slight decrease in the proliferation rate, we did not observe neither an increase in apoptotic cells following dox nor an accumulation of cells in a specific phase of the cell cycle. Therefore, we conclude that dox-induced transposase expression from an IDLV does not lead to pronounced cytotoxic effects, an important difference compared with stable expression from an integrated retroviral vector.

To test the Tet-regulated IDLVs platform in human primary keratinocytes, we transduced the cells with the IDLVTKSB and IDLVrtTA2^S-M2 vectors and scored the activation of the transposase expression upon dox. We observed a clear dox-dependent activation of the transposase demonstrating the possibility to employ this IDLVs platform in primary cells. Unfortunately the all-in-one vector (IDLVTKreg) weakly responded to dox treatment probably due to not correct balance between rtTA2^S-M2 activator and TetOTK responsive element, thereby did not sufficiently support the transposition of GFP expression cassette in primary keratinocytes. In primary cells cotransduced with IDLVTKSB, IDLVrtTA2^S-M2, and IDLV2 vectors the %GFP⁺ cells 5dpt / %GFP⁺ cells 2 dpt × 100 was 12% and had some impact on keratinocytes viability probably due to the total viral load. Noteworthy, the transduction efficiency of the IDLV2 vector was ~2.5-fold lower than transfection efficiency of pSAGFP transposon in HeLa cells. Moreover, we believed that the conformation of transposon template provided by IDLV vector may limit the overall transposition efficiency.^{24,43} Probably circularization of the transposon template, coupled to the regulated transposase system, could increase transposition rate, thus taken into consideration for future applications.

MATERIALS AND METHODS

Plasmids

The pTetOCMVSb plasmid was generated by cloning the TetOminhCMV promoter (from pUHC13.3)⁴⁴ upstream the SB100X coding sequence inserted in the pBlueScript vector (pBS-SB100X). The pTetOTKSB plasmid was obtained by cloning the TetOminTKpromoter²⁷ upstream the SB100X coding sequence (pBS-SB100X). The pSAGFP was described in Turchiano *et al.*³² The pCCL-PGKrtTA2⁵-M2 was kindly provided by Prof. Zappavigna, University of Modena and Reggio Emilia, Italy (IDLVrtTA2⁵-M2). The expression cassette pPGKrtTA2⁵-M2 derived from pCCL-PGKrtTA2⁵-M2 plasmid. The pCCL-TetOTKSB (IDLVTkSB) was achieved by cloning the TetOminTKSB sequence into a pCCL.LV vector. Similarly, was cloned the pCCL-CMVSB100X (IDLVSb). The pCCLT2GFP plasmid (IDLVT2) was generated in two steps: as first the PGKGFPSV40polyA was cloned, according to vector designed shown in Vink *et al.*²⁵ between the T2 IR of the pT2/BH plasmid provided by Prof. Zoltan Ivics (Paul Ehrlich Institute, Langen, Germany), the resulting plasmid was then inserted into a pCCL.LV vector. The pCCLTKSBreg plasmid was achieved by cloning TetOminTKSB in the pCCL-PGKrtTA2⁵-M2 (IDLVTkreg). The pCMVSB100X was kindly provided by Prof. Zoltan Ivics, Paul Ehrlich Institute, Langen Germany.

Cell culture and viral production

HeLa and HEK293T cells were cultured in Dulbecco's modified Eagle's medium supplemented with 10% fetal calf serum, 100 units/ml penicillin and 100 mg/ml streptomycin (Lonza Ltd, Basel Switzerland). Swiss mouse 3T3-J2 cells (a kind gift from Yan Barrandon, EPFL, Lausanne) were grown in Dulbecco's modified Eagle's medium supplemented with 10% donor bovine serum (GIBCO, Thermo Fisher Scientific, Monza Italy), 50 IU/ml penicillin-streptomycin, and 4 mmol/l glutamine. Primary human keratinocytes from foreskin biopsy were plated onto lethally irradiated 3T3-J2 cells and cultured in keratinocyte growth cFAD medium, a Dulbecco's modified Eagle's medium and Ham's F12 media mixture (3:1) containing fetal bovine serum (10%), penicillin-streptomycin (1%), glutamine (2%), insulin (5 µg/ml), adenine (0.18 mmol/l), hydrocortisone (0.4 µg/ml), cholera toxin (0.1 nmol/l), and triiodothyronine (2 nmol/l). After 3 days, EGF at a concentration of 10 ng/ml was added to the culture (KC medium). Keratinocytes were trypsinized at subconfluency and replated onto a new feeder layer.

Viral stocks pseudotyped with the vesicular stomatitis virus G protein were prepared by transient cotransfection of HEK293T-cells with transfer vector, pMD.Lg.pRRc.D64VInt packaging plasmid, pMD2.VSV-G envelope-encoding plasmid, and pRSV-Rev.⁴⁵ Vector particles were concentrated by ultracentrifugation and titrated by HIV-1 Gag p24 immunocapture (Perkin Elmer Life Sciences, Milan, Italy). Titres of IDLVTKSB, IDLVPGKrtTA2-M2, and IDLVT2 vectors are the following respectively: 259 ng/µl p24, 960 ng/µl p24, and 916 ng/µl p24. The titration of IDLVTKreg was based on a dose-escalating (10, 30, 50, and 100 µl) experiment in order to get higher SB activation upon dox treatment and lower toxic effects on the primary keratinocytes. Thus, we used 100 µl to transduce primary keratinocytes. For gammaretroviral vector production (iRVSB), pRSF91SB100X transfer plasmid²³ was cotransfected with MLV-gag-pol³³ and pMD.G plasmids. Vector particles were concentrated by ultracentrifugation.

Transfections and transduction of HeLa cells and primary human keratinocytes

Transfection of HeLa cells. 2.5 × 10⁵ HeLa were transfected with FugeneHD transfection reagent (Roche, S.p.A. Milan, Italy). Each transfection reaction containing 2 µg of DNA was combined with 6 µl of FugeneHD and subsequently mixed by pulse-vortexing for a few seconds. The mixes were thereafter left at room temperature for 10 minutes in order to allow the formation of lipoplexes. After the 10 minutes had expired, each mix was added drop-by-drop to a cell culture sample, which was subsequently incubated at 37°C. The transposon/transposase amounts of plasmid DNA were calculated to respect the stoichiometric ratio of 2:1 in a total quantity of 2 µg. 1 µg of transposon-only plasmid mixed to 1 µg of carrier DNA was used for nontransposed control.

Transduction of HeLa cells. LV or RV transduction was performed by spinoculation at 754 × g for 45' in the presence of polybrene (8 µg/ml). After 6 hours at 37°C, the retro or lenti vectors were replaced with regular medium in presence and in absence of 1 µmol/l dox. The percentage of GFP⁺ cells was determined 2 days and 15–20 days post-transfection/transduction via flow cytometer, then we plotted the %GFP⁺ cells 20 dpt/%GFP⁺ cells 2 dpt × 100 for each sample. The percentage corresponding to the pSAGFP sam-

ple was subtracted to the SB-treated sample. In the transposition experiments, HeLa cells were transfected with 2 µg of pSAGFP transposon using FugeneHD reagent and 16 hours later, cells were transduced with SB-coding viral vectors. HeLa cells transfected only with the transposon plasmid represented the control for transposition experiments.

Transduction of primary human keratinocytes. 1.6 × 10⁵ keratinocytes were LV-transduced in the cFAD medium in the presence of polybrene (8 µg/ml). Amounts of IDLVTKSB, IDLVPGKrtTA2-M2, and IDLVT2 vectors used to transduce primary keratinocytes are the following, respectively: 13,000 ng of p24, 48,000 ng of p24, and 9,160 ng of p24. Then the keratinocytes+vector+polybrene were plated onto lethally irradiated 3T3-J2 cells at 25°C for 30 minutes, subsequently the cells were shifted to 37°C. After 6 hours at 37°C we added cFAD medium to the culture in the presence and in the absence of 1 µmol/l dox. The next day the cFAD medium was replaced with KC medium. Transduced keratinocytes were grown to subconfluency or confluence, trypsinized and replated onto new feeder-layers for future analysis. The percentage of transduced-transposed cells was determined 2–5 days post-transduction via flow cytometer. To discriminate the keratinocytes from the 3T3J2 feeder layer we used the monoclonal Anti-Feeder (APC) antibody mouse conjugated (Miltenyi Biotech S.r.l, Bologna, Italy) according to protocol.

Western blot analysis

In this analysis, 10⁵ HeLa cells were transduced with LV and RV vectors at different multiplicity of infection. 72 hours, 96 hours, and 120 hours post-transduction cells were harvested, washed twice with phosphate-buffered saline and cells lysates were obtained by using Laemmli buffer (Tris-HCL 20 mmol/l pH7.5, ethylene Diamine Tetraacetic Acid (EDTA) 3 mmol/l, Glycerol 20%, sodium dodecyl sulphate (SDS) 2% and β-Mercaptoethanol 5%). Total protein extracts (20 µg) were separated by sodium dodecyl sulphate-polyacrylamide gel electrophoresis (NUPAGE 4–12% BT GEL 1.0 MM12W, Life Technologies, Monza), transferred to nitrocellulose membranes and probed with mouse monoclonal anti-H2A.X-S139P (cat. 16–193 Merck S.p.A. Milano, Italy), mouse monoclonal anti-CyclinB1 (cat. V152 GeneTex, Irvine, CA), mouse monoclonal anti-p53 (cat. sc-126 Santa Cruz Biotechnology, Heidelberg, Germany), mouse monoclonal anti PARP1 (cat. sc-8007 Santa Cruz Biotechnology, Heidelberg, Germany) and antivinulin (cat. V9131, Sigma Aldrich) in Tris-buffered saline with 0.05% Tween (Sigma Aldrich, Milan, Italy) and 5% milk powder (Regilait, Saint Martin Belle Roche France).

Semiquantitative RT-PCR and real time qRT-PCR analysis

Total RNA from the HeLa and keratinocytes transfected/transduced cells was isolated with the RNeasy Mini kit plus (Qiagen, Hilden, Germany), according to the manufacturer's protocol. cDNA was synthesized in a 20 µl reaction using 100 ng total RNA and SuperScript III (Life Technologies).

Semiquantitative reverse-transcriptase polymerase chain reaction (RT-PCR) analysis was performed with the following oligonucleotides.

SB for: 5'-GCCACTCAGCAAGGAAGAAG-3';

SB rev: 5'-GTGTTGGAAGACCCATTTGC-3'

rtTAM2 for: 5'-GACGACAAGGAACTCGCTC-3';

rtTAM2 rev: 5'-TTACCCGGGAGCATGTCAA-3';

GAPDH for: 5'-GACCACAGTCCATGCCATCAC-3';

GAPDH rev: 5'-CCACCACCTGTTGCTGTAG-3'.

PCR cycles: 94°C 30 seconds, 58°C 30 seconds, 72°C 30 seconds.

Real time qRT-PCR was performed as following. Total RNA was isolated from HeLa cells, with the RNeasy Plus Mini Kit (Qiagen). The RNA was reverse transcribed with random primers with the Superscript III reverse transcriptase (Life Technologies). The Real Time Taqman PCR was performed in 96-well plates on the ABI Prism 7900 Sequence Detection System (Applied Biosystems Thermo Fisher Scientific, Milan, Italy) with TaqMan Universal PCR Master Mix and Assays-On-Demand (Applied Biosystems), with a final reaction of 25 µl. The PCR primers and 6-carboxyfluorescein (FAM) probe for glyceraldehyde 3-phosphate dehydrogenase (GAPDH) were purchased from Applied Biosystems. The SB100X transposase levels were measured using custom primers forward SB.2 for 5'-GAAGAAGCCACTGCTCCAAAA-3', reverse primers SB.2 rev 5'-CCCATGTGCAGTTGCAA-3' and probe SB FAM: CATAAGAAAGCCAGACTACGG. All samples were performed in triplicate. The relative expression (RQ value) of the target genes was normalized to the level of GAPDH in the same cDNA by the 2^{-ΔΔCT} quantification.

Quantification of transposon and transposase copies by real-time Taqman PCR (qPCR)

For the quantification of the transposon and transposase copies in transfected/transduced cells, qPCR with the primer pairs specific for GFP (Assay ID Mr04097229_mr, Applied Biosystem) and SB100X (SB.2 forward, reverse, and SB probe described above) were performed.

The quantitative PCR (qPCR) was performed in 96-well plates on the ABI Prism 7900 Sequence Detection System (Applied Biosystems) with TaqMan Universal PCR Master Mix and Assays-On-Demand (Applied Biosystems), with a final reaction of 25 μ l. To normalize the different samples, the same amount of genomic DNA was analyzed by qPCR detecting the GAPDH (Assay ID Hs03929097_g1). As positive control and for the calculation of standard curves, eight serial dilutions of the plasmid standard pCMVSB and pSAGFP (containing 10^9 – 10^2 plasmid copies per 5 μ l) were prepared and subjected to qPCR analysis in triplicate.⁴⁶

Cell proliferation and apoptosis analysis

The inhibition of proliferation was measured by Crystal Violet staining, and the concentration at which cellular growth is inhibited by 50% (IC_{50}) was determined following the indicated time points post transduction.⁴⁷ Briefly, the cell monolayer was fixed with methanol and stained with 0.05% Crystal Violet solution in 20% methanol for 1 hour. After washes, cells were allowed to dry. The incorporated dye was solubilized in acidic isopropanol and determined by absorbance measurement (A_{540nm}). The extracted dye was proportional to cell number. Cells were harvested Propidium-Iodide (PI) and Annexin V staining were performed at 48, 72, 96, and 120 hours after transduction by an FACS CANTO cytometer (BD Biosciences, Milan, Italy).

ACKNOWLEDGMENTS

The authors thank Prof. Zsuzsanna Izsvák (Max Delbruck Center for Molecular Medicine, Berlin, Germany) and Prof. Zoltán Ivics (Paul Ehrlich Institute, Langen, Germany) for kindly providing pCMVSB100X and pT2Venus plasmids. This work was supported by DEBRA international and Italian Ministry of University and Research.

REFERENCES

- Ivics, Z, Hackett, PB, Plasterk, RH and Izsvák, Z (1997). Molecular reconstruction of Sleeping Beauty, a Tc1-like transposon from fish, and its transposition in human cells. *Cell* **91**: 501–510.
- Mátés, L, Chuah, MK, Belay, E, Jerchow, B, Manoj, N, Acosta-Sanchez, A *et al.* (2009). Molecular evolution of a novel hyperactive Sleeping Beauty transposase enables robust stable gene transfer in vertebrates. *Nat Genet* **41**: 753–761.
- Geurts, AM, Yang, Y, Clark, KJ, Liu, G, Cui, Z, Dupuy, AJ *et al.* (2003). Gene transfer into genomes of human cells by the sleeping beauty transposon system. *Mol Ther* **8**: 108–117.
- Zayed, H, Izsvák, Z, Walisko, O and Ivics, Z (2004). Development of hyperactive sleeping beauty transposon vectors by mutational analysis. *Mol Ther* **9**: 292–304.
- Aronovich, EL, Mclvor, RS and Hackett, PB (2011). The Sleeping Beauty transposon system: a non-viral vector for gene therapy. *Hum Mol Genet* **20**(R1): R14–R20.
- Maiti, SN, Huls, H, Singh, H, Dawson, M, Figliola, M, Olivares, S *et al.* (2013). Sleeping beauty system to redirect T-cell specificity for human applications. *J Immunother* **36**: 112–123.
- Johnen, S, Izsvák, Z, Stöcker, M, Harmening, N, Salz, AK, Walter, P *et al.* (2012). Sleeping Beauty transposon-mediated transfection of retinal and iris pigment epithelial cells. *Invest Ophthalmol Vis Sci* **53**: 4787–4796.
- Mann, KM, Ward, JM, Yew, CC, Kovoichich, A, Dawson, DW, Black, MA, *et al.* (2012). Sleeping Beauty mutagenesis reveals cooperating mutations and pathways in pancreatic adenocarcinoma. *Proc Natl Acad Sci USA* **109**: 5934–5941.
- Koso, H, Takeda, H, Yew, CC, Ward, JM, Nariai, N, Ueno, K, *et al.* (2012). Transposon mutagenesis identifies genes that transform neural stem cells into glioma-initiating cells. *Proc Natl Acad Sci USA* **109**: E2998–3007.
- Belay, E, Mátrai, J, Acosta-Sanchez, A, Ma, L, Quattrocchi, M, Mátés, L *et al.* (2010). Novel hyperactive transposons for genetic modification of induced pluripotent and adult stem cells: a nonviral paradigm for coaxed differentiation. *Stem Cells* **28**: 1760–1771.
- Grabundzija, I, Wang, J, Sebe, A, Erdei, Z, Kajdi, R, Devaraj, A *et al.* (2013). Sleeping Beauty transposon-based system for cellular reprogramming and targeted gene insertion in induced pluripotent stem cells. *Nucleic Acids Res* **41**: 1829–1847.
- Kues, WA, Herrmann, D, Barg-Kues, B, Haridoss, S, Nowak-Imialek, M, Buchholz, T *et al.* (2013). Derivation and characterization of sleeping beauty transposon-mediated porcine induced pluripotent stem cells. *Stem Cells Dev* **22**: 124–135.
- Klincumhom, N, Pirity, MK, Berzsenyi, S, Ujhelly, O, Muenthaisong, S, Rungarunlert, S *et al.* (2012). Generation of neuronal progenitor cells and neurons from mouse sleeping beauty transposon-generated induced pluripotent stem cells. *Cell Reprogram* **14**: 390–397.

- Liang, Q, Kong, J, Stalker, J and Bradley, A (2009). Chromosomal mobilization and reintegration of Sleeping Beauty and PiggyBac transposons. *Genesis* **47**: 404–408.
- Izsvák, Z, Ivics, Z and Plasterk, RH (2000). Sleeping Beauty, a wide host-range transposon vector for genetic transformation in vertebrates. *J Mol Biol* **302**: 93–102.
- Izsvák, Z and Ivics, Z (2004). Sleeping beauty transposition: biology and applications for molecular therapy. *Mol Ther* **9**: 147–156.
- Wilber, A, Wangenstein, KJ, Chen, Y, Zhuo, L, Frandsen, JL, Bell, JB *et al.* (2007). Messenger RNA as a source of transposase for sleeping beauty transposon-mediated correction of hereditary tyrosinemia type I. *Mol Ther* **15**: 1280–1287.
- Jin, Z, Maiti, S, Huls, H, Singh, H, Olivares, S, Mátés, L *et al.* (2011). The hyperactive Sleeping Beauty transposase SB100X improves the genetic modification of T cells to express a chimeric antigen receptor. *Gene Ther* **18**: 849–856.
- Yant, SR, Ehrhardt, A, Mikkelsen, JG, Meuse, L, Pham, T and Kay, MA (2002). Transposition from a gutless adeno-transposon vector stabilizes transgene expression in vivo. *Nat Biotechnol* **20**: 999–1005.
- Zhang, W, Muck-Hausl, M, Wang, J, Sun, C, Gebbing, M, Miskey, C *et al.* (2013). Integration profile and safety of an adenovirus hybrid-vector utilizing hyperactive sleeping beauty transposase for somatic integration. *PLoS One* **8**: e75344.
- Zhang, W, Solanki, M, Mütter, N, Ebel, M, Wang, J, Sun, C *et al.* (2013). Hybrid adeno-associated viral vectors utilizing transposase-mediated somatic integration for stable transgene expression in human cells. *PLoS One* **8**: e76771.
- Turunen, TA, Laakkonen, JP, Alasaarela, L, Airenne, KJ and Ylä-Herttua, S (2014). Sleeping Beauty-baculovirus hybrid vectors for long-term gene expression in the eye. *J Gene Med* **16**: 40–53.
- Galla, M, Schambach, A, Falk, CS, Maetzig, T, Kuehle, J, Lange, K *et al.* (2011). Avoiding cytotoxicity of transposases by dose-controlled mRNA delivery. *Nucleic Acids Res* **39**: 7147–7160.
- Moldt, B, Miskey, C, Staunstrup, NH, Gogol-Döring, A, Bak, RO, Sharma, N *et al.* (2011). Comparative genomic integration profiling of Sleeping Beauty transposons mobilized with high efficacy from integrase-defective lentiviral vectors in primary human cells. *Mol Ther* **19**: 1499–1510.
- Vink, CA, Gaspar, HB, Gabriel, R, Schmidt, M, Mclvor, RS, Thrasher, AJ *et al.* (2009). Sleeping beauty transposition from nonintegrating lentivirus. *Mol Ther* **17**: 1197–1204.
- Hackett, PB, Largaespada, DA, Switzer, KC and Cooper, LJ (2013). Evaluating risks of insertional mutagenesis by DNA transposons in gene therapy. *Transl Res* **161**: 265–283.
- Recchia, A, Perani, L, Sartori, D, Olgiati, C and Mavilio, F (2004). Site-specific integration of functional transgenes into the human genome by adeno-AAV hybrid vectors. *Mol Ther* **10**: 660–670.
- Agha-Mohammadi, S, O'Malley, M, Etemad, A, Wang, Z, Xiao, X and Lotze, MT (2004). Second-generation tetracycline-regulatable promoter: repositioned tet operator elements optimize transactivator synergy while shorter minimal promoter offers tight basal leakiness. *J Gene Med* **6**: 817–828.
- Urlinger, S, Baron, U, Thellmann, M, Hasan, MT, Bujard, H, and Hillen, W (2000). Exploring the sequence space for tetracycline-dependent transcriptional activators: novel mutations yield expanded range and sensitivity. *Proc Natl Acad Sci USA* **97**: 7963–7968.
- Vigna, E, Cavaliere, S, Ailles, L, Geuna, M, Loew, R, Bujard, H *et al.* (2002). Robust and efficient regulation of transgene expression *in vivo* by improved tetracycline-dependent lentiviral vectors. *Mol Ther* **5**: 252–261.
- Lamartina, S, Roscilli, G, Rinaudo, CD, Sporeno, E, Silvi, L, Hillen, W *et al.* (2002). Stringent control of gene expression *in vivo* by using novel doxycycline-dependent transactivators. *Hum Gene Ther* **13**: 199–210.
- Turchiano, G, Latella, MC, Gogol-Döring, A, Cattoglio, C, Mavilio, F, Izsvák, Z *et al.* (2014). Genomic analysis of Sleeping Beauty transposon integration in human somatic cells. *PLoS One* **9**: e112712.
- Schambach, A, Bohne, J, Baum, C, Hermann, FG, Egerer, L, von Laer, D *et al.* (2006). Woodchuck hepatitis virus post-transcriptional regulatory element deleted from X protein and promoter sequences enhances retroviral vector titer and expression. *Gene Ther* **13**: 641–645.
- Bell, JB, Aronovich, EL, Schreifels, JM, Beadnell, TC and Hackett, PB (2010). Duration of expression and activity of Sleeping Beauty transposase in mouse liver following hydrodynamic DNA delivery. *Mol Ther* **18**: 1796–1802.
- Aiuti, A, Biasco, L, Scaramuzza, S, Ferrua, F, Cicalese, MP, Baricordi, C *et al.* (2013). Lentiviral hematopoietic stem cell gene therapy in patients with Wiskott-Aldrich syndrome. *Science* **341**: 1233151.
- Biffi, A, Montini, E, Lorioli, L, Cesani, M, Fumagalli, F, Plati, T *et al.* (2013). Lentiviral hematopoietic stem cell gene therapy benefits metachromatic leukodystrophy. *Science* **341**: 1233158.
- Cartier, N, Hacein-Bey-Abina, S, Von Kalle, C, Bognères, P, Fischer, A, Cavazzana-Calvo, M *et al.* (2010). [Gene therapy of x-linked adrenoleukodystrophy using hematopoietic stem cells and a lentiviral vector]. *Bull Acad Natl Med* **194**: 255–64; discussion 264.
- Cavazzana-Calvo, M, Payen, E, Negre, O, Wang, G, Hehir, K, Fusil, F *et al.* (2010). Transfusion independence and HMG2 activation after gene therapy of human β -thalassaemia. *Nature* **467**: 318–322.
- Deniger, DC, Yu, J, Huls, MH, Figliola, MJ, Mi, T, Maiti, SN *et al.* (2015). Sleeping Beauty transposition of chimeric antigen receptors targeting receptor tyrosine kinase-like

- orphan Receptor-1 (ROR1) into diverse memory T-cell populations. *PLoS One* **10**: e0128151.
40. Singh, H, Moyes, JS, Huls, MH and Cooper, LJ (2015). Manufacture of T cells using the Sleeping Beauty system to enforce expression of a CD19-specific chimeric antigen receptor. *Cancer Gene Ther* **22**: 95–100.
41. Singh, H, Huls, H, Kebriaei, P and Cooper, LJ (2014). A new approach to gene therapy using Sleeping Beauty to genetically modify clinical-grade T cells to target CD19. *Immunol Rev* **257**: 181–190.
42. Ahler, E, Sullivan, WJ, Cass, A, Braas, D, York, AG, Bensinger, SJ *et al.* (2013). Doxycycline alters metabolism and proliferation of human cell lines. *PLoS One* **8**: e64561.
43. Cai, Y and Mikkelsen, JG (2014). Driving DNA transposition by lentiviral protein transduction. *Mob Genet Elements* **4**: e29591.
44. Gossen, M, and Bujard, H (1992). Tight control of gene expression in mammalian cells by tetracycline-responsive promoters. *Proc Natl Acad Sci US A* **89**: 5547–5551.
45. Coluccio, A, Miselli, F, Lombardo, A, Marconi, A, Malagoli Tagliazucchi, G, Gonçalves, MA *et al.* (2013). Targeted gene addition in human epithelial stem cells by zinc-finger nuclease-mediated homologous recombination. *Mol Ther* **21**: 1695–1704.
46. Aurnhammer, C, Haase, M, Muether, N, Hausl, M, Rauschhuber, C, Huber, I *et al.* (2012). Universal real-time PCR for the detection and quantification of adeno-associated virus serotype 2-derived inverted terminal repeat sequences. *Hum Gene Ther Methods* **23**: 18–28.
47. Basile, V, Belluti, S, Ferrari, E, Gozzoli, C, Ganassi, S, Quaglino, D *et al.* (2013). bis-Dehydroxy-Curcumin triggers mitochondrial-associated cell death in human colon cancer cells through ER-stress induced autophagy. *PLoS One* **8**: e53664.



This work is licensed under a Creative Commons Attribution-NonCommercial-NoDerivs 4.0 International License. The images or other third party material in this article are included in the article's Creative Commons license, unless indicated otherwise in the credit line; if the material is not included under the Creative Commons license, users will need to obtain permission from the license holder to reproduce the material. To view a copy of this license, visit <http://creativecommons.org/licenses/by-nc-nd/4.0/>

© F Cocchiarella *et al.* (2016)

Supplementary Information accompanies this paper on the *Molecular Therapy—Methods & Clinical Development* website (<http://www.nature.com/mtm>)